

Foveation dynamics in congenital nystagmus IV: vergence

Louis F. Dell'Osso, Johannes Van Der Steen, Robert M. Steinman & Han Collewijn

Documenta Ophthalmologica
The Journal of Clinical
Electrophysiology and Vision - The
Official Journal of the International
Society for Clinical Electrophysiology
and Vision

ISSN 0012-4486

Doc Ophthalmol
DOI 10.1007/s10633-019-09738-y



Official Publication of the International Society for Clinical Electrophysiology and Vision
May 2008 · Volume 116 · Number 3

Documenta
Ophthalmologica
The Journal of Clinical Electrophysiology of Vision

The journal cover features a large, stylized, light blue wave-like graphic on the left side. In the center, there are four scientific plots: two topographic maps (spatial frequency tuning curves) and two corresponding electrophysiological waveforms. The topographic maps show color-coded peaks and valleys, with color bars indicating values in dB and mV/deg². The waveforms show oscillatory patterns with scale bars for voltage (200 mV and 500 mV) and time (0-100 ms).

Free color
Illustrations!

Submit Manuscripts:
<http://www.editorialmanager.com/doop>

Springer
ISSN: 0012-4486

Your article is protected by copyright and all rights are held exclusively by This is a U.S. Government work and not under copyright protection in the US; foreign copyright protection may apply. This e-offprint is for personal use only and shall not be self-archived in electronic repositories. If you wish to self-archive your article, please use the accepted manuscript version for posting on your own website. You may further deposit the accepted manuscript version in any repository, provided it is only made publicly available 12 months after official publication or later and provided acknowledgement is given to the original source of publication and a link is inserted to the published article on Springer's website. The link must be accompanied by the following text: "The final publication is available at link.springer.com".



ORIGINAL RESEARCH ARTICLE

Foveation dynamics in congenital nystagmus IV: vergence

Louis F. Dell'Osso · Johannes Van Der Steen · Robert M. Steinman · Han Collewijn

Received: 15 August 2019 / Accepted: 12 November 2019

© This is a U.S. Government work and not under copyright protection in the US; foreign copyright protection may apply 2019

Abstract

Purpose To evaluate foveation dynamics and characteristics of vergence eye movements during fixation of static targets at different distances and while tracking a target moving in depth in a subject with congenital nystagmus (CN).

Method Eye movements of a well-studied subject with CN were recorded using the magnetic search coil technique and analyzed using the OMtools software, including the eXpanded Nystagmus Acuity Function (NAFX).

Results Both the phase planes and NAFX values during fixation of targets at various near distances were equivalent to those during fixation of a far target. When applied to vergence data, the NAFX values (“binocular” NAFX) were higher than for the individual eye data. Vergence tracking of targets moving in depth was demonstrated and was accurate for targets moving at speeds up to $\sim 35^\circ/\text{sec}$.

Conclusions Target foveation qualities during fixation of targets at various near distances were equivalent to that during fixation of a far target. Stereo discrimination was limited by the foveation quality of the eye with the higher NAFX waveform. Foveation period slopes during vergence tracking demonstrated vergence movements despite the ongoing CN

L. F. Dell'Osso, Robert M. Steinman and Han Collewijn—
Professor Emeritus

L. F. Dell'Osso
Daroff-Dell'Osso Ocular Motility Laboratory, Louis Stokes Cleveland, Department of Veterans Affairs Medical Center, CASE Medical School, Case Western Reserve University and University Hospitals Case Medical Center, 10701 East Boulevard, Cleveland, OH 44106, USA

L. F. Dell'Osso
Departments of Neurology, Case Western Reserve University and University Hospitals Case Medical Center, Cleveland, OH, USA

L. F. Dell'Osso (✉)
Departments of Biomedical Engineering, Case Western Reserve University and University Hospitals Case Medical Center, Cleveland, OH, USA
e-mail: lfd@case.edu

J. Van Der Steen · H. Collewijn (✉)
Department of Neuroscience, ErasmusMC, Rotterdam, The Netherlands

R. M. Steinman (✉)
Department of Psychology, University of Maryland, College Park, MD, USA

oscillation. Similar to what we found with fixation, pursuit, and the vestibulo-ocular systems, these findings establish that vergence in both static and dynamic viewing conditions functions normally in the presence of the CN oscillation.

Keywords Congenital nystagmus · Infantile nystagmus syndrome · Vergence · Tracking

Glossary

General terms

CN	Congenital nystagmus
INS	Infantile nystagmus syndrome
IPD	Interpupillary distance
NAFX	Expanded nystagmus acuity function

CN waveforms

JRef	Jerk right with extended foveation
PPfs	Pseudo-pendular with foveating saccades

Calculated terms

LEH	Left eye horizontal
LEH_err	Left eye horizontal error
REH	Right eye horizontal
REH_err	Right eye horizontal error
TDIST	Target distance
TDIST_vel	Target distance velocity
TVRG	Target vergence
TVRG_vel	Target vergence velocity
VRG	Vergence
VRG_err	Vergence error
VRG_vel	Vergence velocity

Introduction

The effect of nystagmus on fixation, smooth pursuit, and the vestibulo-ocular response has always been a source of interest and concern to both researchers and clinicians. In our original studies of the binocular foveation dynamics of a subject with congenital nystagmus (CN), we demonstrated that despite the ongoing oscillation: (i) the fixation of stationary distant and near targets was normal; (ii) tracking of horizontally moving targets was normal; and (iii) fixation of stationary distant targets during head movements was also normal [1–3]. Note that although “CN” has long been replaced by “Infantile Nystagmus Syndrome (INS)” [4], for historical consistency with the original three papers (cited above), the former

(old fashioned) terminology will be used in this paper. We examined the foveation dynamics of the same subject during binocular fixation of static targets at different distances and during tracking of a target moving in depth (i.e., the dynamics of vergence).

Methods

Recording

The data were recorded by means of a phase-detecting revolving magnetic field technique in the Laboratory of R.M. Steinman. The sensor coils consisted of nine turns of fine copper wire imbedded in an annulus of silicone rubber molded to adhere to the eye by suction. The signals were digitized at 488 Hz with a resolution of 16 bits. The system's sensitivity was less than one minute of arc (minarc), with linearity of one part in 14,014 and drift of 0.2–0.3 minarc/hour. Noise was less than two minarc, and eye position was stored to the nearest minarc. Further details of this specific system can be found elsewhere [5, 6]. Note that the original data were taken in minarc and were converted in this paper to degrees (°), conforming to the analysis software we used.

Protocol

Written consent was obtained from the 46-year-old male subject before the testing. All test procedures were carefully explained to the subject before the experiment began and were reinforced with verbal commands during the trials. The subject, with sensor coils attached to both eyes, sat near the center of the revolving magnetic field and viewed the easily visible LED targets at various distances in a dimly lit room. The subject bit on a custom-made bite board to prevent head movements. The LED subtended less than 0.03° of visual angle.

Static targets

Data were taken during convergence on far and near targets. The room light could be adjusted from dim down to blackout to minimize extraneous visual stimuli. An experiment consisted of from one to twenty trials, each lasting under a minute. Time was allowed between trials to permit the subject to rest. Trials were kept this short to guard against boredom because CN intensity is known to decrease with

inattention. Vergence targets ranged from the farthest target at 5.8 m to the nearest one at 8.3 cm, yielding vergence angles between 0.6° (far) and 39.1° (near) for this subject.

Targets moving in depth

Vergence tracking was conducted during binocular viewing of a target (a white nail head) that was manually moved by the experimenter. The subject could not predict the target velocities used during each trial but each trial began with a target motion toward the subject starting from an initial position of 32.8 cm. The target distance was calculated from the voltage output of a lever and coil.

Relevant clinical data

The subject had CN but did not have strabismus or amblyopia. His best-corrected binocular visual acuity was 20/40 (0.500), which improved to 20/25 (0.800) with base-out prisms added to his refraction. His stereo acuity, tested with either Randot or the Titmus “Fly” method, was 20–40 s of arc.

Analysis

The analysis of the digitized eye movement data was conducted using the OMtools software, including the eXpanded Nystagmus Acuity Function (NAFX). The NAFX (an expansion of the NAF) is a mathematical function that provides a numerical output that is linearly proportional to the decimal equivalent of Snellen acuity [7]. It uses time, position, and velocity measures of foveation quality and an expandable position vs. velocity “foveation” window to arrive at that number, that is, it calculates the position and velocity standard deviations of the CN waveform’s foveation periods in a given interval of fixation (2–5 s).

Both the software and instructions for its use may be downloaded from our website, omlab.org. Horizontal, rightward version movements of both eyes were positive, as were convergence movements. Ocular vergence was calculated from the horizontal eye movement data as left eye minus right eye, and the target vergence was given by $2(\arctan [IPD/20TDIST])$, where the IPD = 59 mm and TDIST is

target distance in cm. Phase planes (position vs. velocity) plots were also used in the analysis.

Results

Data were taken during static fixation of targets at various distances and also during vergence tracking of targets moving at various velocities toward and away from the subject.

Fixation on static targets at different distances

During static fixation on the far target (5.8 m), each eye is converged by 0.3° . This served as the baseline to which the convergence on nearer targets was compared. Figure 1 (top) shows an interval containing such a fixation. The foveation periods of both eyes were at their respective converged positions ($\pm 0.3^\circ$), and the vergence during these foveation periods was 0.6° . The NAFX output highlights the intervals satisfying the NAFX position and velocity criteria for each eye as well as vergence, which is shown in the center panel. Due to the low CN amplitude, in addition to the four foveation periods of the CN waveforms that are at 0° , the highlighted intervals show some data obtained during two other small intervals in each eye also satisfied the NAFX position and velocity criteria. The slight disconjugacies in the embedded foveating and braking saccades of the pseudo-pendular with foveating saccades (PPfs) and a single cycle of jerk right with extended foveation [JRef] waveforms introduced noise into the vergence trace. As the interval after the foveating saccade of the JRef cycle shows, the vergence trace without noise would be a horizontal line centered at 0.6° . Despite this noise, the NAFX function determined that all data points satisfied the position and velocity criteria of the foveation window (i.e., the whole vergence trace was emphasized in the NAFX output). The bottom panel shows phase plane trajectories of both eyes and vergence in retinocentric coordinates (i.e., with the average vergence angle removed) during fixation on the far target. Each of the foveation periods fell within the foveation window, as did most of the vergence trajectory. The vergence phase plane was emphasized and colored to allow better visualization of this small, well-foveated trajectory.

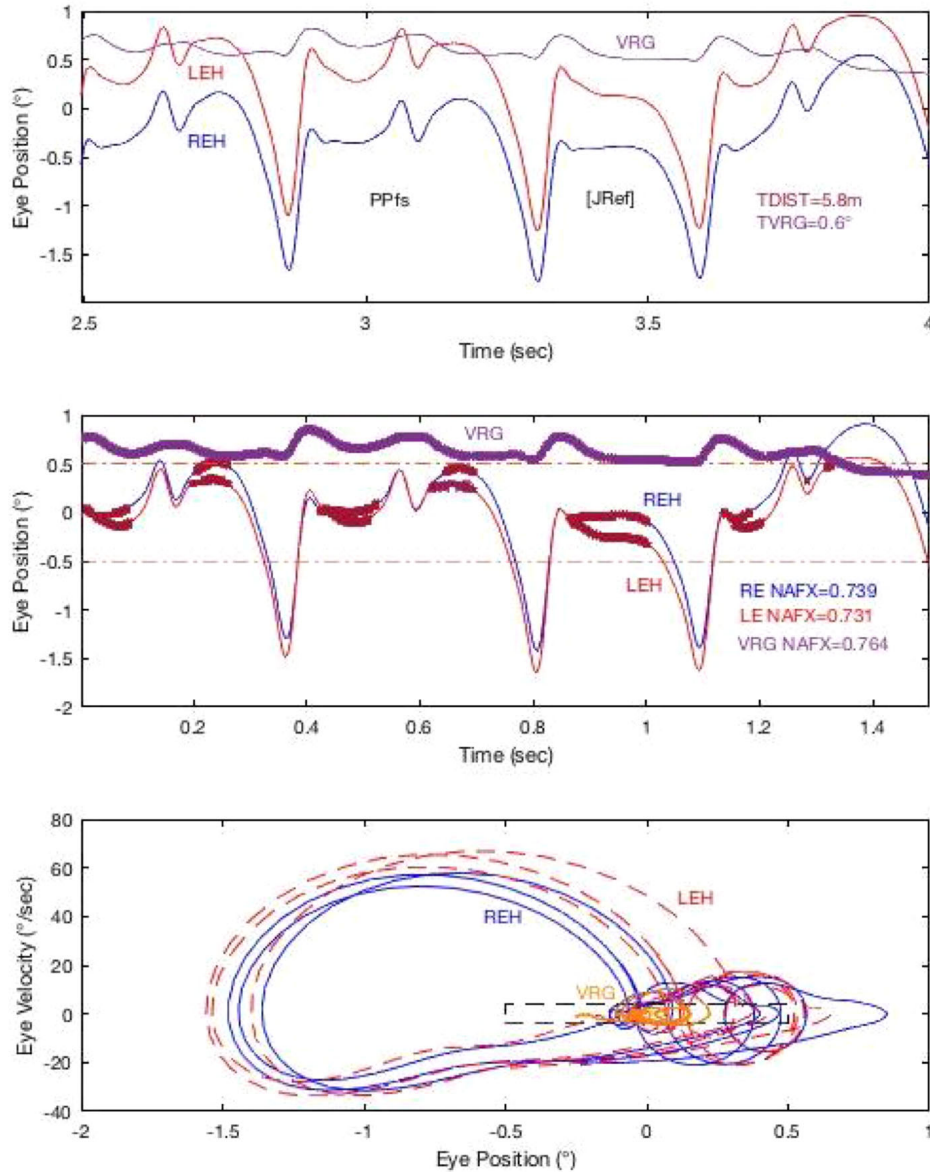


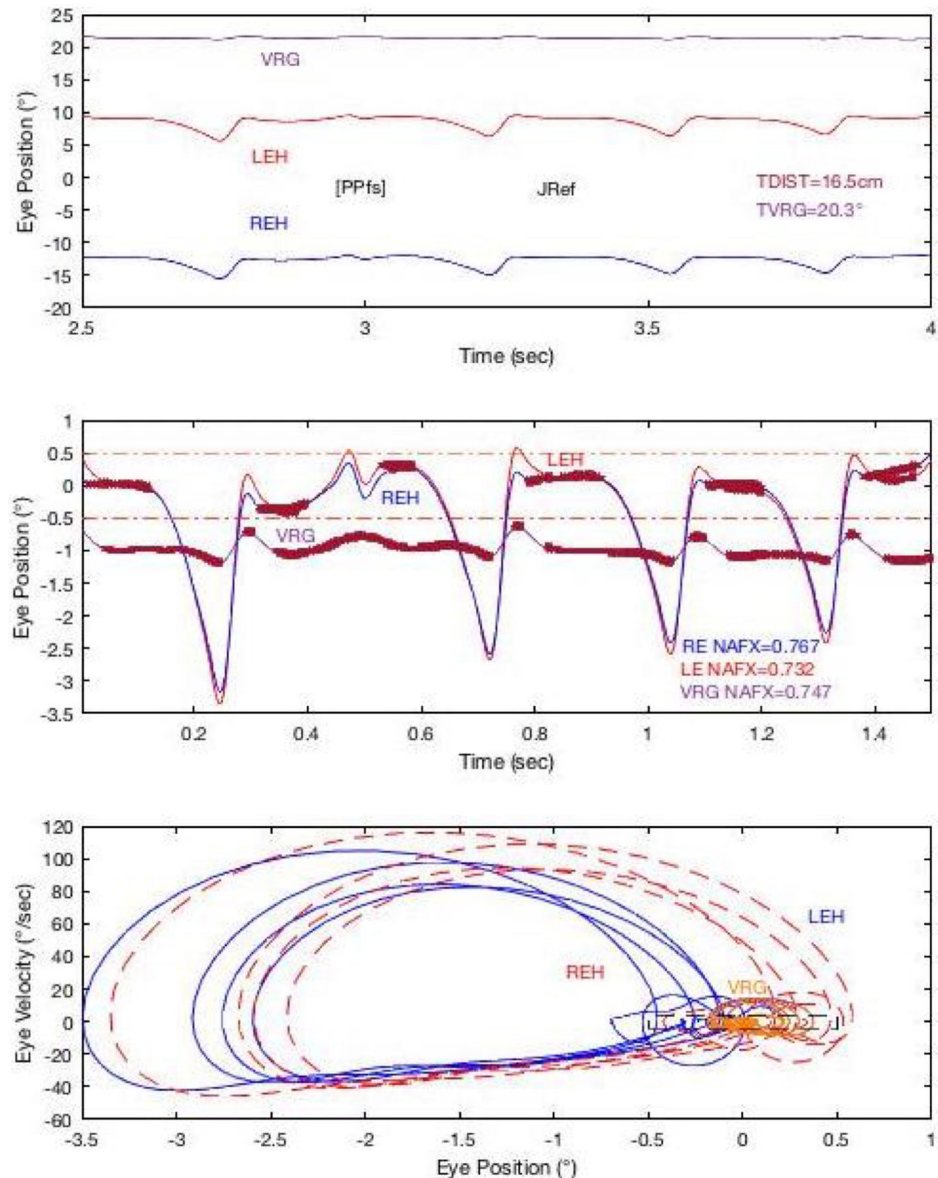
Fig. 1 Eye position and vergence during static fixation on a far (5.8 m) target (top panel) and NAFX-identified foveation periods (emphasized) in each eye and in the vergence trace (center panel). Phase planes of both eyes and vergence are shown in the bottom panel. The emphasized vergence trace (center panel) was shifted up to its vergence value for clarity. The average vergence was 0.6°. In this and the following figures: predominant and single-cycle “[]” waveforms are identified, target distances, vergences, and NAFX values for each eye and vergence data are provided; the dot-dashed lines in the center

plot indicate the position boundaries of the NAFX foveation window; LEH, left eye horizontal position in °; REH, right eye horizontal position in °; VRG, vergence in °; TDIST, target distance; TVRG, target vergence; PPfs, pseudo-pendular with foveating saccades; JRef, jerk right with extended foveation; and in the phase plane plots, LEH is shown dashed for clarity; the dashed rectangle is the ±0.5° by ±4°/sec foveation window; and the VRG and VRG_err phase planes are shown in a lighter color and emphasized for clarity

Figure 2 shows the data and analysis for fixation on a near, static target at 16.5 cm, which is less than half of normal reading distance. The top panel shows an interval of such fixation. The foveation periods of each eye are at their respective converged position (~ 9.5

and ~ 12.5°), and the vergence trace during these foveation periods was ~ 22°. The NAFX output highlights intervals satisfying the NAFX position and velocity criteria for each eye and vergence, as shown in the center panel. As the highlighted intervals

Fig. 2 Eye position and vergence during static fixation on a near (16.5 cm) target (top panel) and NAFX-identified foveation periods (emphasized) in each eye and in the vergence trace (center panel). Phase planes of both eyes and vergence are shown in the bottom panel. The average vergence was 22°. The emphasized vergence trace (center) was shifted down by 1° for clarity

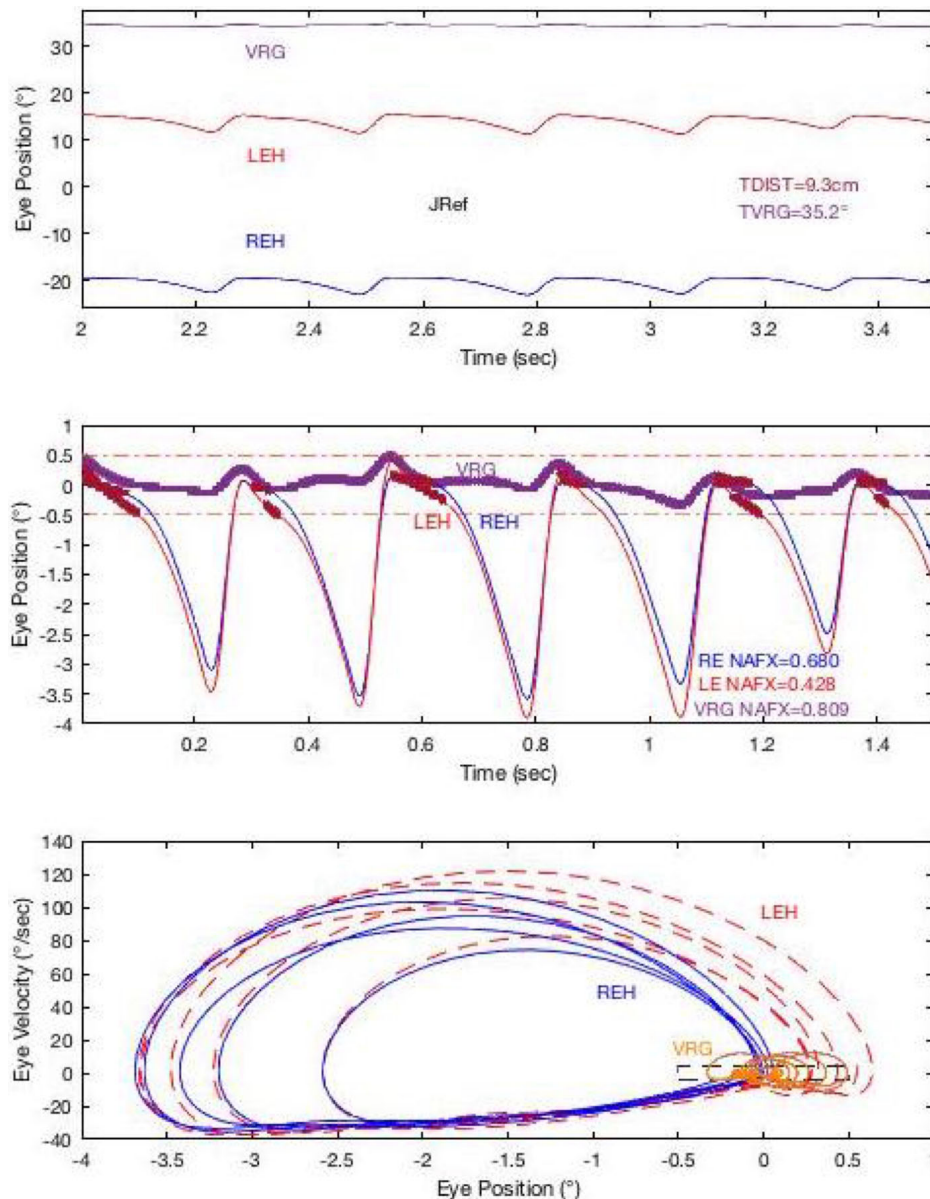


show, in addition to the six foveation periods of the CN waveforms that are at 0°, data obtained during the other small intervals in each eye satisfied the NAFX position and velocity criteria. The slight disconjugacies in the embedded foveating saccades of the JRef and single cycle of [PPfs] waveforms produced contamination in the vergence trace. Without the disconjugacy-produced noise, the vergence trace would otherwise be a horizontal line centered at ~ 22°. Again, the NAFX function determined that all data points satisfied the position and velocity criteria of the foveation window. The bottom panel shows phase plane trajectories of both eyes and vergence in

retinocentric coordinates during fixation on this near target. As during fixation on a far target, each of the foveation periods fell within the foveation window, as did most of the vergence trajectory.

Figure 3 shows the data and analysis for fixation on a near, static target at 9.3 cm, which was close to maximum convergence without a break in fusion. The top panel shows an interval with this kind of fixation. The foveation periods of each eye were at their respective converged position (~ 16 & ~ 19°), and the vergence trace during these foveation periods was ~ 35°. The NAFX output highlights the intervals that satisfy the NAFX position and velocity criteria for

Fig. 3 Eye position and vergence during static fixation on a near (9.3 cm) target (top panel) and NAFX-identified foveation periods (emphasized) in each eye and in the vergence trace (center panel). Phase planes of both eyes and vergence are shown in the bottom panel. The average vergence was 35°



each eye as well as for vergence, which is shown in the center panel. As the highlighted intervals show, in addition to the six foveation periods of the CN waveforms that were at 0° , data during other small intervals in each eye also satisfied the NAFX position and velocity criteria. The slight disconjugacies in the embedded foveating saccades of the jerk right with extended foveation JRef waveform produced noise in the vergence trace. Without the disconjugacy-produced contamination, the vergence trace would otherwise be a horizontal line centered at $\sim 35^\circ$. Again, the NAFX function determined that all data points

satisfied the position and velocity criteria of the foveation window. The bottom panel shows phase plane trajectories of both eyes and vergence in retinocentric coordinates during fixation on this near target. As during fixation on a far target, each of the foveation periods fell within the foveation window, as did most of the vergence trajectory.

Foveation accuracy for static targets at different distances

We calculated the NAFX values for each eye during fixation of static targets between 9.3 cm and 36.6 cm and compared them to the NAFX during fixation of the distant target (5.8 m). Data from the nearest target (8.3 cm) were not used since the subject had difficulty maintaining binocular alignment on that target. As Fig. 4 shows, the NAFX values for the vergence data: trended upward with binocular convergence, are uniformly higher; and more tightly fit the trend line than those from the eye data. The single data points available to calculate the NAFX for the best eye were too variable to display the NAFX increase with convergence that has been demonstrated for this subject [1, 8]. Also, since the target presentation was random, (i.e., not presented in either a monotonically increasing or decreasing vergence manner), the data could not demonstrate the hysteresis later found when targets were sequentially presented in such a manner (i.e., NAFX values during divergence are greater than

during convergence) [9] tracking of a target moving in depth.

Vergence tracking of a target moving in depth

The vergence tracking response of the subject to a target moving slowly ($\leq 8^\circ/\text{sec}$) toward him is shown in Fig. 5. The foveation periods of each eye were initially horizontal (slope = 0), while the target was stationary (0–1 s). However, as the target moved toward the subject, the foveation periods assume velocities in adduction (positive slopes for the left eye and negative slopes for the right eye). As the overall eye position traces show, the CN waveform of each eye slowly adducted; that is, the left eye moved rightward and the right eye, leftward. The result was convergence that, as the vergence trace shows, closely followed the vergence angle of the target. Note that the CN waveforms of the two eyes essentially disappeared from the vergence trace because of the conjugate nature of the CN and the definition of vergence as the difference between the left and right eye positions ($\text{VRG} = \text{LEH} - \text{REH}$, which is positive for

Fig. 4 NAFX vs. Vergence Angle plots for the best eye and the vergence data during binocular fixation of static targets at different distances

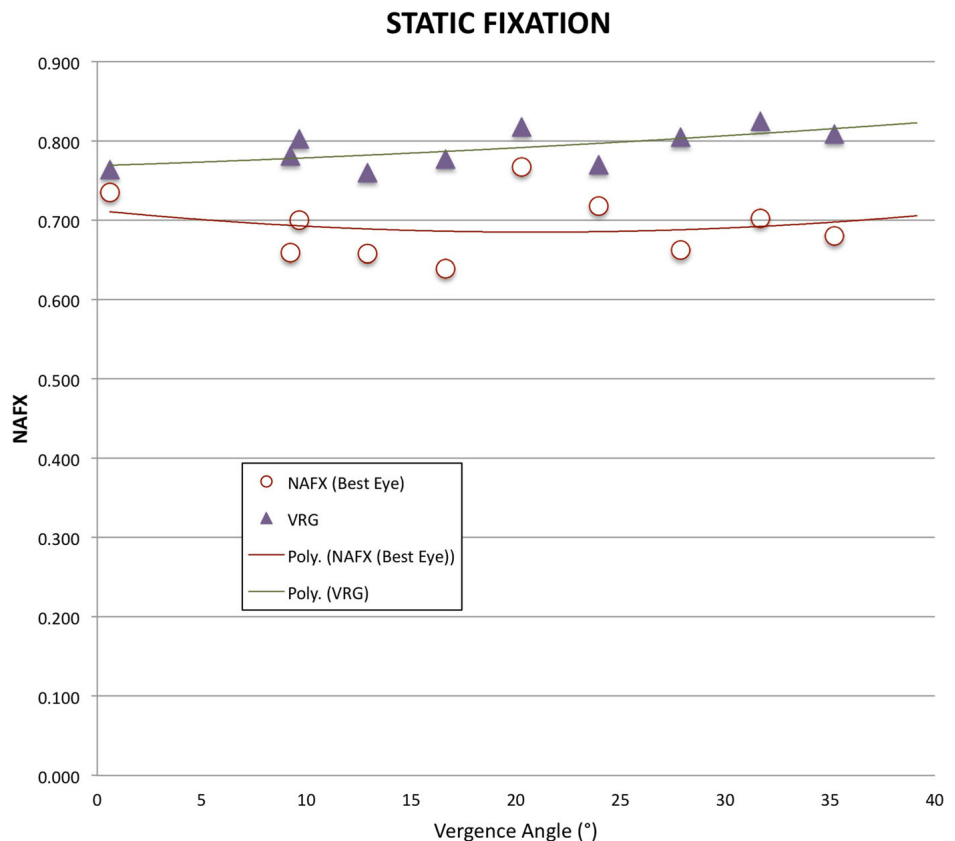
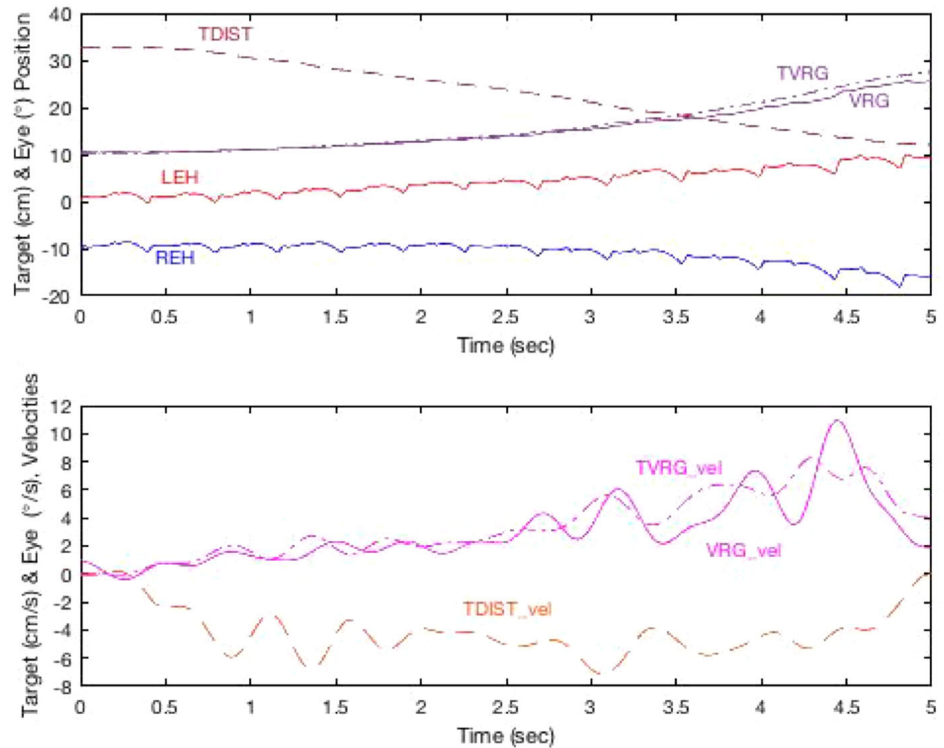


Fig. 5 Target and eye position (top panel) and velocity (bottom panel) plots during slow ($\leq 8^\circ/\text{sec}$) vergence tracking. In this and the following figures, TDIST, target distance in cm; TVRG, target vergence in $^\circ$; TDIST_vel, target velocity in cm/sec; TVRG_vel, target vergence velocity in $^\circ/\text{sec}$; and VRG_vel, vergence velocity in $^\circ/\text{sec}$



convergence based on the convention of rightward motion being defined as positive). Because vergence is an arctangent function of distance, even these segments where the target distance change was linear (i.e., target velocity was constant) did not result in a linear vergence input to the vergence system. Because both the target and eye vergence traces contained uncorrelated noise (see the low-pass filtered oscillations in the bottom traces), attempts to form a gain function by dividing target vergence velocity by eye vergence velocity did not yield usable results. True vergence gain could only be determined by the quotient of target to eye vergence velocities evaluated during the foveation periods of each CN cycle or by graphical techniques using linear approximations for each segment [10]; this is equivalent to what we previously demonstrated for horizontal smooth pursuit and vestibulo-ocular responses [2, 3].

Figure 6 shows the vergence tracking response at a higher convergence velocity ($\leq 43^\circ/\text{sec}$). In addition to the observations evident for the slow vergence tracking response, we also found a damping of the CN waveforms with convergence, leaving almost pure vergence movements, and a saturation of the amount of vergence at the nearest positions of the target. Also,

during the divergence portion of the response, the eye vergence trace again mimicked the target stimulus at low velocities but fell behind and saturated as target vergence velocity increased. These observations were exacerbated at very fast vergence velocities ($\leq 108^\circ/\text{sec}$), (see Fig. 7). The vergence response fell behind the target and saturated for most of the response. These high velocities mimic those found in normal control subjects (see reference 17, Table 1).

Figure 8 shows the phase planes of each eye, vergence, and target vergence (top) and of the vergence error for each eye and for binocular vergence (bottom) from the data taken during slow vergence tracking ($\text{TVRG_vel} \leq 8^\circ/\text{sec}$). The time plots of the vergence error of each eye are shown in the center panel. As the overlapping phase plane trajectories of both eyes in top panel show, each eye adducted from its initial position only when the target moved inward after the first second of the record. The vergence trace of the eyes followed that of the target. The center panel shows that there was no vergence error during the static target phase (0–1 s), and the maximum vergence error was 1–1.5 $^\circ$ for most of the record. The error phase planes were formed in the same manner as we previously applied to smooth pursuit and vestibulo-

Fig. 6 Target and eye position (top panel) and velocity (bottom panel) plots during rapid ($\leq 43^\circ/\text{sec}$) vergence tracking

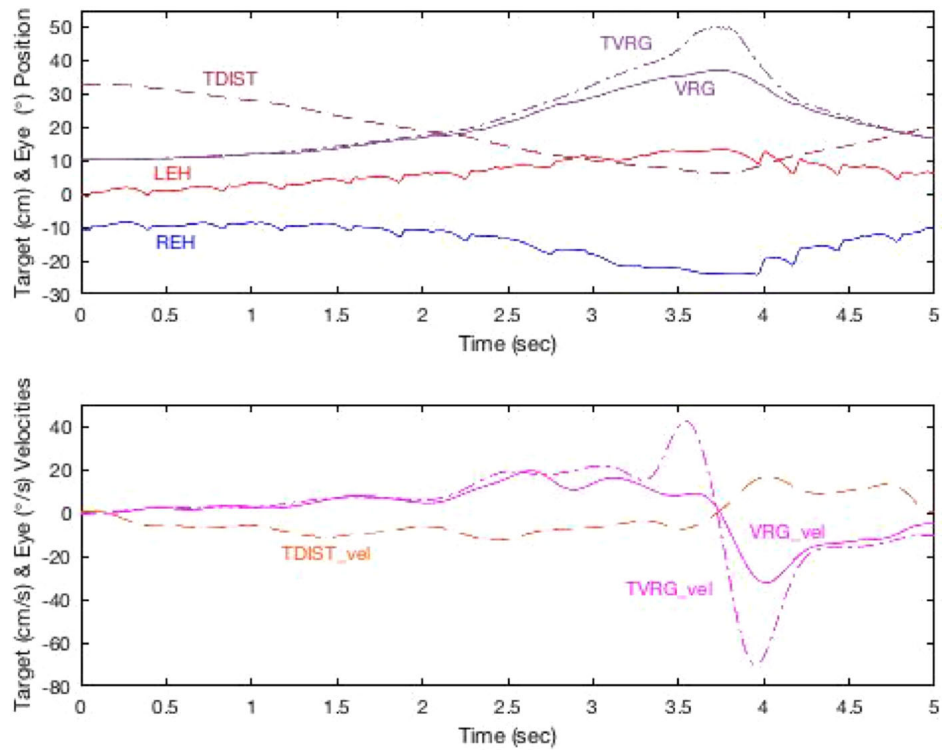
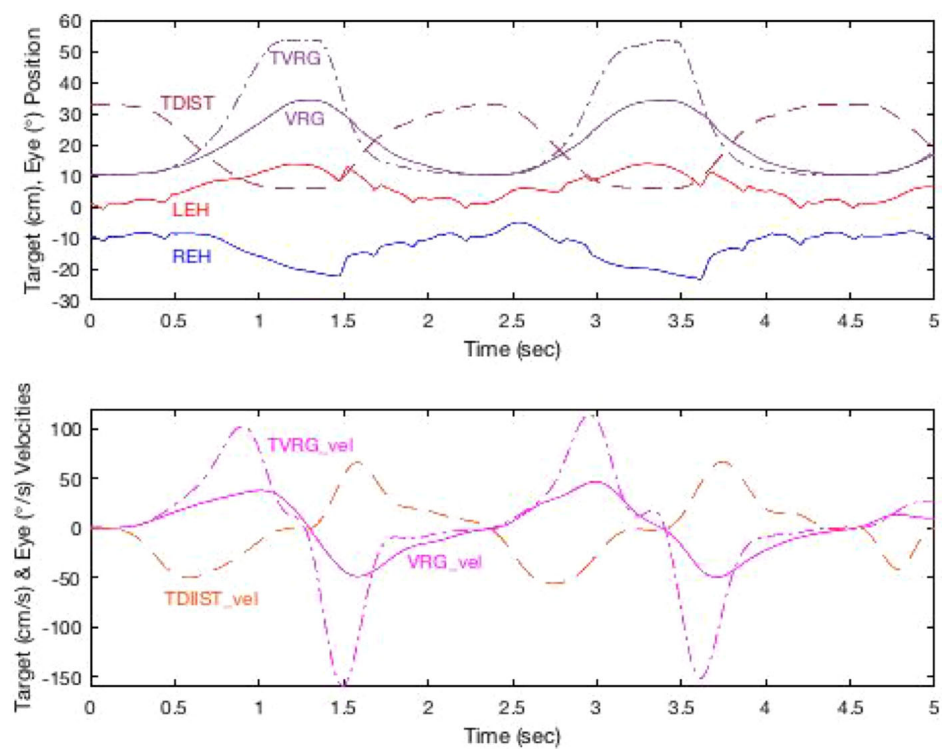


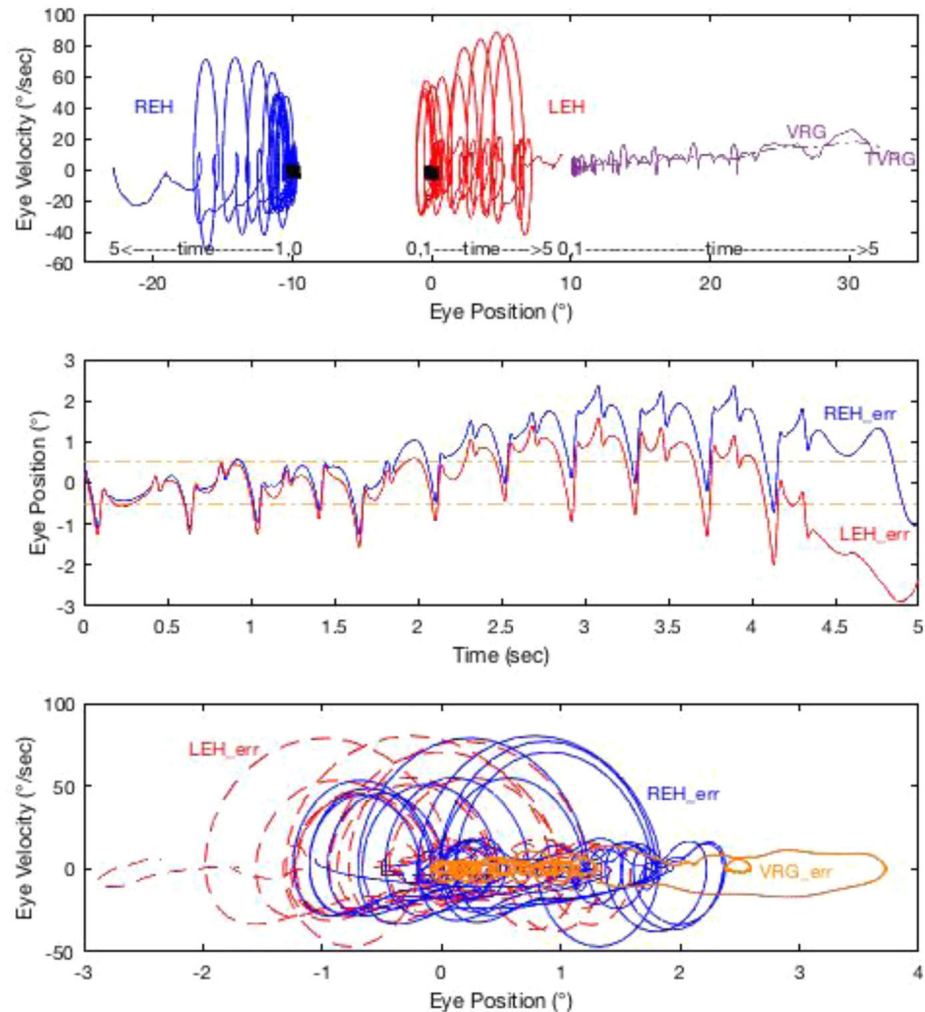
Fig. 7 Target and eye position (top panel) and velocity (bottom panel) plots during very fast ($\leq 108^\circ/\text{sec}$) vergence tracking



ocular data [2, 3]. Specifically, $REH_{err} = REH + TVRG/2$, $LEH_{err} = LEH - TVRG/2$, and $VRG_{err} = VRG - TVRG$. The phase plane

trajectories in Fig. 8 can be compared to the error phase planes in those publications as well as to the static vergence phase planes in Figs. 1, 2 and 3.

Fig. 8 Phase planes of each eye and vergence (top panel) during slow ($\leq 8^\circ/\text{sec}$) vergence tracking. The dark rectangles in the top plot are the respective foveation windows for each eye during the first second when target position was static. To aid in understanding, starting and ending time indications of the data in the center panel are provided for each phase plane trajectory. The center panel shows the time plot of the vergence error of each eye and bottom panel, the vergence error of each eye and of the binocular vergence. REH_err, right eye horizontal/vergence error in $^\circ$; LEH_err, left eye horizontal/vergence error in $^\circ$; VRG_err, binocular vergence error in $^\circ$



Discussion

The authors of this paper spent the week of September 14–18, 1987, in the Laboratory of Dr. R.M. Steinman studying the foveation dynamics of congenital nystagmus (CN), which was present in one of us (L.F. Dell’Osso). Data were taken of: (i) the fixation of stationary distant and near targets (days 1 and 2); (ii) tracking of horizontally moving targets (day 3); (iii) fixation of stationary distant targets during head movements (day 4); and (iv) fixation and tracking of targets at different distances (day 5). Analysis of the data from the first four days resulted in three publications [1–3]. The vergence data taken on day 5 were preserved and transferred through several generations of computers and operating systems over the next 32 years but remained unanalyzed until recently; these

data provided the observations and conclusions about vergence contained in the present paper.

To the authors’ knowledge, the eye movement data taken in 1987 of a subject with CN fixating stationary targets at different distances (i.e., different static vergence angles) were the first such data. A study of the effects of vergence on the CN waveform and foveation quality did not appear until two decades later [9]. However, dynamic vergence tracking (i.e., “depth-pursuit”) data in CN had never before (nor since) been documented; its analysis in this paper is also unique.

Vergence tracking and the relative contributions of blur and disparity have been extensively studied using several approaches. These included: random-dot stereograms [11, 12]; electronically generated or projected targets [13–16]; and real targets [17, 18].

In our paradigm, we used natural targets and disparity, blur, size, and awareness of the arrangement; they all contributed to the vergence response. Therefore, the findings of studies employing real targets in a more natural setting are most relevant to this paper. They produced accurate ($\pm 1\text{--}2^\circ$) and fast ($\leq 100^\circ/\text{sec}$) vergence responses that were improved when the subject moved the target rather than the experimenter [17]. Studies of symmetric and asymmetric vergence step responses found them to be mediated by saccades [18]. Monocular vergence (i.e., with one eye occluded) was slower and inaccurate compared to binocular vergence.

Fixation on static targets at different distances

As is evident from both the NAFX and scan path panels in Figs. 1, 2 and 3, high-quality foveation by both eyes was achieved during fixation of static targets, regardless of their distance from the subject. That is, there was no abnormal fixation disparity. Thus, activation of the vergence system did not interfere with, and in some cases improved, target foveation quality despite any waveform changes that occurred.

The “Binocular” NAFX

The NAFX function is a measure of the motor effects of ocular oscillations on potential visual acuity [7, 19, 20]. It identifies the data intervals that satisfy position and velocity criteria (i.e., the foveation periods of CN waveforms) necessary for high spatial acuity and its value is equivalent to the decimal value of Snellen acuity. The NAFX has been used in subjects with CN, with or without associated afferent visual deficits, to assess their potential acuity before therapy (i.e., to distinguish the motor and sensory components of measured acuity) and to predict the post-therapy improvements in peak acuity, high-acuity gaze-angle range, and target acquisition time [21, 22]. In our prior paper, we also documented the foveation dynamics during fixation on a far target while viewing through base-out prisms [1]. By applying the NAFX to the vergence data of this subject (see Figs. 1, 2, 3, 4), we now provide a measure of the impact of CN disconjugacy on vergence alignment and, therefore, on binocular fusion and stereopsis. In this subject, as Figs. 1, 2, 3 show, the “binocular” NAFX was higher

than that measured in either eye. Thus, the subject's stereopsis would not be limited by CN disconjugacy but rather by the NAFX of each eye. This novel use of the NAFX on the calculated vergence data may provide insights into the effects of disjunctive oscillations on binocular fusion and stereopsis (both absolute and relative) similar to those conducted on normal subjects [11, 12, 23–25].

Vergence tracking of moving targets at different distances

Examination of the vergence tracking data (Figs. 5, 6, 7, 8) revealed accurate vergence tracking at low vergence velocities, reduction in vergence speed and tracking accuracy at higher velocities, and a saturation for this subject at vergence values above $\sim 35^\circ$. Age-matched control subjects saturated around $60^\circ/\text{sec}$, while younger subjects saturated at $30^\circ/\text{sec}$; those were average speeds where peak speeds could be twice as fast (see reference 17, p. 424 and reference 18, Figs. 5 and 6).

In the first three studies of foveation dynamics in CN, we employed a precursor to the NAFX (the NFF, Nystagmus Foveation Function) and phase planes to analyze fixation of a static far target, pursuit of a horizontally moving target, and the effects of head motion on fixation of a static far target [1–3]. We demonstrated that despite the ocular oscillations, the fixation, smooth pursuit, and vestibulo-ocular subsystems functioned normally. From the analysis of data taken during fixation of static targets at different distances and tracking of targets moving in depth, we can now additionally conclude that the vergence fixation and tracking subsystems also function normally despite the CN oscillations.

Acknowledgements This work was supported in part by the Office of Research and Development, Medical Research Service, Department of Veterans Affairs.

Compliance with ethical standards

Conflict of interest The authors declare that they have no conflicts of interest.

Statement of human rights All procedures performed in studies involving human participants were approved by the appropriate institutional committee and were in accordance with the ethical standards of the University of Maryland and with the

1964 Helsinki declaration and its later amendments or comparable ethical standards.

Statement on the welfare of animals This article does not contain any studies with animals performed by any of the authors.

Informed consent Informed consent was obtained from the individual participant included in the study.

References

- Dell'Osso LF, Van der Steen J, Steinman RM, Collewijn H (1992) Foveation dynamics in congenital nystagmus I: fixation. *Doc Ophthalmol* 79:1–23
- Dell'Osso LF, Van der Steen J, Steinman RM, Collewijn H (1992) Foveation dynamics in congenital nystagmus II: smooth pursuit. *Doc Ophthalmol* 79:25–49
- Dell'Osso LF, Van der Steen J, Steinman RM, Collewijn H (1992) Foveation dynamics in congenital nystagmus III: vestibulo-ocular reflex. *Doc Ophthalmol* 79:51–70
- CEMAS_Working_Group (2001) A National Eye Institute Sponsored Workshop and Publication on The Classification of Eye Movement Abnormalities and Strabismus (CEMAS). In The National Eye Institute Publications. www.nei.nih.gov/news/statements/cemas.pdf
- Collewijn H, Erkelens CJ, Steinman RM (1988) Binocular co-ordination of human horizontal saccadic eye movements. *J Physiol* 404:157–182
- Collewijn H, Erkelens CJ, Steinman RM (1988) Binocular co-ordination of human vertical saccadic eye movements. *J Physiol* 404:183–197
- Dell'Osso LF, Jacobs JB (2002) An expanded nystagmus acuity function: intra- and intersubject prediction of best-corrected visual acuity. *Doc Ophthalmol* 104:249–276
- Dell'Osso LF, Gauthier G, Liberman G, Stark L (1972) Eye movement recordings as a diagnostic tool in a case of congenital nystagmus. *Am J Optom Arch Am Acad Optom* 49:3–13
- Serra A, Dell'Osso LF, Jacobs JB, Burnstine RA (2006) Combined gaze-angle and vergence variation in infantile nystagmus: two therapies that improve the high-visual acuity field and methods to measure it. *Invest Ophthalmol Vis Sci* 47:2451–2460
- Dell'Osso LF (1986) Evaluation of smooth pursuit in the presence of congenital nystagmus. *Neuro ophthalmol* 6:383–406
- Erkelens CJ, Collewijn H (1985) Eye movements and stereopsis during dichoptic viewing of moving random-dot stereograms. *Vision Res* 25:1689–1700
- Pobuda M, Erkelens CJ (1993) The relationship between absolute disparity and ocular vergence. *Biol Cyber* 68:221–228
- Erkelens CJ, Regan D (1986) Human ocular vergence movements induced by changing size and disparity. *J Physiol* 379:145–169
- Erkelens CJ (1987) Adaptation of ocular vergence to stimulation with large disparities. *Exp Brain Res* 66:507–516
- Wismeijer DA, Erkelens CJ (2009) The effect of changing size on vergence is mediated by changing disparity. *J Vis* 9:1–10
- Neveu P, Philippe M, Priot A-E, Fuchs P, Roumes C (2012) Vergence tracking: a tool to assess oculomotor performance in stereoscopic displays. *J Eye Movement Res* 51:1–8
- Erkelens CJ, Van der Steen J, Steinman RM, Collewijn H (1989) Ocular vergence under natural conditions. I. Continuous changes of target distance along the median plane. *Proc Roy Soc Lond B (Biol)* 236:417–440
- Erkelens CJ, Steinman RM, Collewijn H (1989) Ocular vergence under natural conditions. II. Gaze shifts between real targets differing in distance and direction. *Proc Roy Soc Lond B (Biol)* 236:441–465
- Dell'Osso LF (2005) Using the NAFX for eye-movement fixation data analysis and display. *OMLAB Report* 111005:1–7
- Jacobs JB, Dell'Osso LF (2010) Extending the expanded nystagmus acuity function for vertical and multiplanar data. *Vision Res* 50:271–278
- Wang Z, Dell'Osso LF, Jacobs JB, Burnstine RA, Tomsak RL (2006) Effects of tenotomy on patients with infantile nystagmus syndrome: foveation improvement over a broadened visual field. *JAAPOS* 10:552–560
- Wang ZI, Dell'Osso LF (2007) A review of the tenotomy nystagmus surgery: origin, mechanism, and general efficacy. *Neuro-Ophthalmol* 31:157–165
- Regan D, Erkelens CJ, Collewijn H (1986) Necessary conditions for the perception of motion in depth. *Invest Ophthalmol Vis Sci* 27:584–597
- Erkelens CJ, Collewijn H (1991) Control of vergence: gating among disparity inputs by voluntary target selection. *Exp Brain Res* 87:671–678
- Erkelens CJ (2011) A dual visual-local feedback model of the vergence eye movement system. *J Vision* 21:1–14

Publisher's Note Springer Nature remains neutral with regard to jurisdictional claims in published maps and institutional affiliations.